

## PAPER

# Frequency-Domain Equalization for Single-Carrier Space-Time Block Coded Transmit Diversity in a High Mobility Environment

Hiroyuki MIYAZAKI<sup>†a)</sup>, *Student Member* and Fumiyuki ADACHI<sup>†</sup>, *Fellow*

**SUMMARY** Single-carrier (SC) transmission with space-time block coded (STBC) transmit diversity can achieve good bit error rate (BER) performance. However, in a high mobility environment, the STBC codeword orthogonality is distorted and as consequence, the BER performance is degraded by the interference caused by the orthogonality distortion of STBC codeword. In this paper, we proposed a novel frequency-domain equalization (FDE) for SC-STBC transmit diversity in doubly selective fading channel. Multiple FDE weight matrices, each associated with a different code block, are jointly optimized based on the minimum mean square error (MMSE) criterion taking into account not only channel frequency variation but also channel time variation over the STBC codeword. Computer simulations confirm that the proposed robust FDE achieves BER performance superior to conventional FDE, which was designed based on the assumption of a quasi-static fading.

**key words:** *space-time block coding, frequency-domain equalization, doubly selective fading*

## 1. Introduction

Single-carrier with minimum mean square error based frequency-domain equalization (SC-FDE) [1]–[3] can be used to overcome the channel frequency selectivity problem and obtain large frequency diversity gain while achieving lower peak-to-average power ratio (PAPR) than orthogonal frequency-division multiplexing (OFDM) [4]–[6]. The combined use of space-time block coding (STBC) transmit diversity can further improve the transmission performance [7]–[9]. SC-STBC transmit diversity combined with receive FDE (called as frequency-domain space time transmit diversity (FD-STTD) [9]) requires the channel state information (CSI) at only the receiver while obtaining both spatial and frequency diversity gain. Therefore, FD-STTD transmission is suitable for uplink (mobile terminal → base station) transmission.

In the next generation mobile communication systems, broadband and high quality data services are demanded even in a high mobility environment. However, in a high mobility environment, the STBC codeword orthogonality tends to be distorted and as consequence, the BER performance is severely degraded due to the orthogonality distortion of STBC codeword (below, we refer to it as STBC codeword interference) [10]. Iterative interference cancellation (I<sup>2</sup>C) was proposed to mitigate the orthogonality distortion [11], [12].

However, I<sup>2</sup>C requires high computational complexity at the receiver.

In this paper, we propose a novel FDE, called as the robust FDE, suitable for SC-STBC diversity in doubly selective fading channel. In the proposed robust FDE, Multiple FDE weight matrices, each associated with a different coded block, are used within a STBC codeword. Furthermore, multiple FDE weight matrices are jointly optimized based on the minimum mean square error (MMSE) criterion taking into account not only channel frequency variation but also channel time variation over the STBC codeword (note that the conventional FDE weight is optimized assuming that the channel does not change within a STBC codeword [9]). We show by computer simulation that the proposed robust FDE can tolerate higher Doppler frequency than the conventional FDE [9] in FD-STTD transmission. Then we show that the proposed robust FDE achieves almost the same BER performance as I<sup>2</sup>C [11], [12] with lower computational complexity.

The rest of this paper is organized as follows. Section 2 presents the transmitter/receiver structures and signal representation for FD-STTD transmission. The robust FDE for high mobility environment is derived in Sect. 3. The computer simulation results are discussed in Sect. 4, and finally, Sect. 5 offers conclusion.

*Notation:*  $E[\cdot]$ ,  $[\cdot]^T$ ,  $[\cdot]^H$  denote the ensemble average operation, the transpose operation and the Hermitian transpose operation, respectively.  $\|\mathbf{x}\|$  is the norm of vector  $\mathbf{x}$ .

## 2. SC-STBC Diversity with Robust FDE

Throughout the paper, the symbol spaced discrete-time signal representation is used. We consider that the transmitter and receiver have  $N_t$  antennas and  $N_r$  antennas, respectively.

Figure 1 illustrates the transmitter and receiver structures in FD-STTD transmission. In the transmitter,  $J \times N_c$  data modulated symbols are divided into  $J$  blocks of  $N_c$  symbols each, where  $J$  denotes the number of transmit blocks before STBC encoding and  $N_c$  is the fast Fourier transform (FFT) block size. The time-domain transmit signal is transformed into the frequency-domain transmit signal by  $N_c$ -point FFT.  $J$  frequency-domain transmit signal blocks are encoded into a STBC codeword, which consists of  $N_t$  streams of  $Q$  frequency-domain coded signal blocks each, by STBC encoding, where  $Q$  denotes the number of coded transmit signal blocks after STBC encoding. Repre-

Manuscript received June 1, 2015.

Manuscript revised December 20, 2015.

<sup>†</sup>The authors are with the Department of Communications Engineering, Graduate School of Engineering, Tohoku University, Sendai-shi, 980-8579 Japan.

a) E-mail: miyazaki@mobile.ecei.tohoku.ac.jp  
DOI: 10.1587/transcom.2015EBP3230

sending the  $j$ th frequency-domain transmit signal blocks as  $\{D_j(k) : k = 0, \dots, N_c - 1\}$ , the  $q$ th coded transmit signal vector  $\mathbf{X}_q(k) = [X_q(0, k), \dots, X_q(N_t - 1, k)]^T$  can be expressed as

$$\begin{bmatrix} \mathbf{X}_0^T(k) \\ \mathbf{X}_1^T(k) \end{bmatrix} = \begin{bmatrix} D_0(k) & D_1(k) \\ -D_1^*(k) & D_0^*(k) \end{bmatrix}, \quad \text{if } N_t = 2, \quad (1a)$$

$$\begin{bmatrix} \mathbf{X}_0^T(k) \\ \mathbf{X}_1^T(k) \\ \mathbf{X}_2^T(k) \\ \mathbf{X}_3^T(k) \end{bmatrix} = \begin{bmatrix} D_0(k) & D_1(k) & D_2(k) \\ -D_1^*(k) & D_0^*(k) & 0 \\ -D_2^*(k) & 0 & D_0^*(k) \\ 0 & -D_2^*(k) & D_1^*(k) \end{bmatrix}, \quad \text{if } N_t = 3, \quad (1b)$$

$$\begin{bmatrix} \mathbf{X}_0^T(k) \\ \mathbf{X}_1^T(k) \\ \mathbf{X}_2^T(k) \\ \mathbf{X}_3^T(k) \end{bmatrix} = \begin{bmatrix} D_0(k) & D_1(k) & D_2(k) & 0 \\ -D_1^*(k) & D_0^*(k) & 0 & D_2(k) \\ -D_2^*(k) & 0 & D_0^*(k) & -D_1(k) \\ 0 & -D_2^*(k) & D_1^*(k) & D_0(k) \end{bmatrix}, \quad \text{if } N_t = 4, \quad (1c)$$

In FD-STTD, The combination of  $J$ ,  $Q$ , and the STBC coding rate  $R_{STBC} = J/Q$  is determined by the number  $N_t$  of the transmit antennas summarized in Table 1 [9]. After STBC encoding, the frequency-domain STBC codeword is transformed back to the time-domain STBC codeword by  $N_c$ -point inverse FFT (IFFT). After inserting cyclic prefix (CP) into the beginning of each block, the generated STBC codeword is transmitted over  $Q$  time-slots.

At the receiver, after CP removal, the time-domain received STBC codeword is transformed into the frequency-domain STBC codeword by  $N_c$ -point FFT. The  $q$ th frequency-domain received signal vector  $\mathbf{Y}_q(k) = [Y_q(0, k), \dots, Y_q(N_r - 1, k)]^T$  can be expressed as

$$\mathbf{Y}_q(k) = \sqrt{\frac{2P}{N_t(J/Q)}} \mathbf{H}_q(k) \mathbf{X}_q(k) + \mathbf{\Pi}_q(k), \quad (2)$$

where  $\mathbf{H}_q(k)$  is the  $N_r \times N_t$  channel transfer function matrix in the  $q$ th time-slot and  $H_q(n_r, n_t, k)$  is the element of channel transfer function matrix in the  $n_r$ -th row and the  $n_t$ -th column.  $P$  denotes the transmit power.  $\mathbf{\Pi}_q(k) = [\Pi_q(0, k), \dots, \Pi_q(N_r - 1, k)]^T$  is the noise vector and  $\Pi_q(N_r, k)$  is the zero mean complex valued additive white Gaussian noise (AWGN) having variance  $2N_0/T_s$  with  $N_0$  and  $T_s$  being the single-sided power spectrum density of AWGN and the symbol duration, respectively. Then, the robust FDE is performed to the received STBC codeword. The  $q$ th received signal vector,  $\hat{\mathbf{Y}}_q(k) = [\hat{Y}_q(0, k), \dots, \hat{Y}_q(N_r - 1, k)]^T$ , after the robust FDE is given as

$$\hat{\mathbf{Y}}_q(k) = \mathbf{W}_q(k) \mathbf{Y}_q(k), \quad (3)$$

where  $\mathbf{W}_q(k) = [\mathbf{W}_q^T(0, k), \dots, \mathbf{W}_q^T(N_t - 1, k)]^T$  with  $\mathbf{W}_q(n_t, k) = [W_q(n_t, 0, k), \dots, W_q(n_t, N_r - 1, k)]$  is the  $q$ th  $N_t \times N_r$  robust FDE weight matrix. The STBC decoding is performed to obtain the decoded frequency-domain signal. The  $j$ th decoded frequency-domain signal,

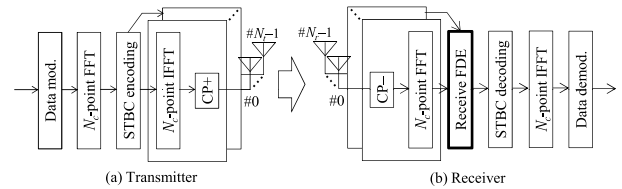


Fig. 1 Transmitter/receiver structure.

Table 1 Relationship among  $N_t$ ,  $J$ ,  $Q$  and  $R_{STBC}$ .

No. of transmit antennas $N_t$	No. of transmit blocks $J$	No. of coded blocks $Q$	STBC coding rate $R_{STBC}$
2	2	2	2
3	3	4	3/4
4	3	4	3/4

$\{\hat{D}_j(k) : k = 0, \dots, N_c - 1, j = 0, \dots, J - 1\}$ , is given as

$$\begin{bmatrix} \hat{D}_0(k) \\ \hat{D}_1(k) \end{bmatrix} = \begin{bmatrix} \hat{Y}_0(0, k) + \hat{Y}_1^*(1, k) \\ \hat{Y}_0(1, k) - \hat{Y}_1^*(0, k) \end{bmatrix}, \quad \text{if } N_t = 2, \quad (4a)$$

$$\begin{bmatrix} \hat{D}_0(k) \\ \hat{D}_1(k) \\ \hat{D}_2(k) \end{bmatrix} = \begin{bmatrix} \hat{Y}_0(0, k) + \hat{Y}_1^*(1, k) + \hat{Y}_2^*(2, k) \\ \hat{Y}_0(1, k) - \hat{Y}_1^*(0, k) + \hat{Y}_3^*(2, k) \\ \hat{Y}_0(2, k) - \hat{Y}_2^*(0, k) - \hat{Y}_3^*(1, k) \end{bmatrix}, \quad \text{if } N_t = 3, \quad (4b)$$

$$\begin{bmatrix} \hat{D}_0(k) \\ \hat{D}_1(k) \\ \hat{D}_2(k) \end{bmatrix} = \begin{bmatrix} \hat{Y}_0(0, k) + \hat{Y}_1^*(1, k) + \hat{Y}_2^*(2, k) + \hat{Y}_3^*(3, k) \\ \hat{Y}_0(1, k) - \hat{Y}_1^*(0, k) - \hat{Y}_2^*(3, k) + \hat{Y}_3^*(2, k) \\ \hat{Y}_0(2, k) + \hat{Y}_1^*(3, k) - \hat{Y}_2^*(0, k) - \hat{Y}_3^*(1, k) \end{bmatrix}, \quad \text{if } N_t = 4, \quad (4c)$$

The decoded frequency-domain signal is transformed back to the time-domain signal by  $N_c$ -point IFFT and finally, data demodulation is carried out.

### 3. Robust FDE for a High Mobility Environment

In this paper, we derive the robust FDE weight matrices for SC-STBC diversity in a high mobility environment. The robust FDE weight matrices, each associated with a different coded block, are jointly optimized so as to minimize the mean square error (MSE) between the transmit signal before STBC encoding and the received signal after STBC decoding taking into account not only channel frequency variation but also channel time variation over the STBC codeword, i.e. under the assumption given as  $\mathbf{H}_0(k) \neq \dots \neq \mathbf{H}_{Q-1}(k)$ . Below, we introduce the derivation of the robust FDE when  $N_t = 2$ . The derivation of the robust FDE when  $N_t = 3, 4$  is denoted in Appendix.

The MSE,  $e$ , in FD-STTD transmission is defined as

$$e = \sum_{j=0}^{J-1} \sum_{k=0}^{N_c-1} E \left[ \left| D_j(k) - \sqrt{\frac{2P}{N_t(J/Q)}} \hat{D}_j(k) \right|^2 \right]. \quad (5)$$

The  $n_t$ th column vector of  $\mathbf{H}_q(k)$  is represented as  $\mathbf{H}_q(n_t, k) = [H_q(0, n_t, k), \dots, H_q(N_r - 1, n_t, k)]^T$ . Then, from Eq. (1a), (2), (3) and (4a),  $e$  can be rewritten as

$$\begin{aligned}
e = & \sum_{k=0}^{N_c-1} \left\{ \left| \mathbf{W}_0(0, k) \mathbf{H}_0(0, k) + \mathbf{H}_1^H(1, k) \mathbf{W}_1^H(1, k) - 1 \right|^2 \right. \\
& \left. + \left| \mathbf{W}_0(1, k) \mathbf{H}_0(1, k) + \mathbf{H}_1^H(0, k) \mathbf{W}_1^H(0, k) - 1 \right|^2 \right\} \\
& + N_t \left( \frac{J}{Q} \right) \left( \frac{P}{N} \right)^{-1} \sum_{q=0}^{Q-1} \sum_{n_t=0}^{N_t-1} \sum_{k=0}^{N_c-1} \left\| \mathbf{W}_q(n_t, k) \right\|^2 \quad (6) \\
& + \sum_{k=0}^{N_c-1} \left\{ \left| \mathbf{W}_0(0, k) \mathbf{H}_0(1, k) - \mathbf{H}_1^H(0, k) \mathbf{W}_1^H(1, k) \right|^2 \right. \\
& \left. + \left| \mathbf{W}_0(1, k) \mathbf{H}_0(0, k) - \mathbf{H}_1^H(1, k) \mathbf{W}_1^H(0, k) \right|^2 \right\}
\end{aligned}$$

The first term is the contribution of the residual ISI after the robust FDE due to the channel frequency selectivity and the second term is the contribution of the noise. The third term is the contribution of the residual STBC codeword interference caused by the channel time selectivity. The robust FDE weights are jointly optimized so as to minimize the MSE given as

$$\left\{ \begin{array}{l} \mathbf{W}_0(0, k), \mathbf{W}_0(1, k) \\ \mathbf{W}_1(0, k), \mathbf{W}_1(1, k) \end{array} \right\} = \text{argmin } e. \quad (7)$$

By solving  $\partial e / \partial \mathbf{W}_0(0, k) = \mathbf{0}, \dots, \partial e / \partial \mathbf{W}_{Q-1}(N_t-1, k) = \mathbf{0}$ , the robust MMSE-FDE weights are obtained as

$$\left\{ \begin{array}{l} \mathbf{W}_0(0, k) = \frac{\mathbf{H}_0^H(0, k) - \mathbf{H}_0^H(1, k) (\tilde{H}_2(k) / \tilde{H}_1(k))}{\tilde{H}_0(k) - \left( |\tilde{H}_2(k)|^2 / \tilde{H}_1(k) \right)} \\ \mathbf{W}_0(1, k) = \frac{\mathbf{H}_0^H(1, k) - \mathbf{H}_0^H(0, k) (\tilde{H}_3(k) / \tilde{H}_0(k))}{\tilde{H}_1(k) - \left( |\tilde{H}_3(k)|^2 / \tilde{H}_0(k) \right)} \\ \mathbf{W}_1(0, k) = \frac{\mathbf{H}_1^H(0, k) - \mathbf{H}_1^H(1, k) (\tilde{H}_3(k) / \tilde{H}_0(k))}{\tilde{H}_1(k) - \left( |\tilde{H}_3(k)|^2 / \tilde{H}_0(k) \right)} \\ \mathbf{W}_1(1, k) = \frac{\mathbf{H}_1^H(1, k) - \mathbf{H}_1^H(0, k) (\tilde{H}_2(k) / \tilde{H}_1(k))}{\tilde{H}_0(k) - \left( |\tilde{H}_2(k)|^2 / \tilde{H}_1(k) \right)} \end{array} \right. \quad (8)$$

where

$$\left\{ \begin{array}{l} \tilde{H}_0(k) = \|\mathbf{H}_0(0, k)\|^2 + \|\mathbf{H}_1(1, k)\|^2 + N_t \left( \frac{J}{Q} \right) \left( \frac{P}{N} \right)^{-1} \\ \tilde{H}_1(k) = \|\mathbf{H}_0(1, k)\|^2 + \|\mathbf{H}_1(0, k)\|^2 + N_t \left( \frac{J}{Q} \right) \left( \frac{P}{N} \right)^{-1} \\ \tilde{H}_2(k) = \mathbf{H}_0^H(0, k) \mathbf{H}_0(1, k) - \mathbf{H}_1^H(0, k) \mathbf{H}_1(1, k) \\ \tilde{H}_3(k) = \mathbf{H}_0^H(1, k) \mathbf{H}_0(0, k) - \mathbf{H}_1^H(1, k) \mathbf{H}_1(0, k) \end{array} \right. \quad (9)$$

and  $N = N_0/T_s$  is the noise power. The second terms in denominator and numerator in Eq. (8) contribute to suppress the STBC codeword interference. When the channel time variation over a STBC codeword is sufficiently slow ( $\mathbf{H}_0(k) \approx, \dots, \approx \mathbf{H}_{Q-1}(k)$ ), Eq. (8) corresponds to the conventional FDE weight which was designed based on the assumption of a quasi-static fading [9].

#### 4. Computer Simulation

We evaluate, by computer simulation, the BER performance when using FD-STTD transmission with the proposed robust FDE. QPSK data modulation is considered. FFT block size

$N_c$  and CP length  $N_g$  are set to  $N_c = 128$  symbols and  $N_g = 16$  samples, respectively. The channel is assumed to be a time and frequency-selective Rayleigh fading channel having symbol spaced  $L = 16$  path uniform power delay profile. In this paper, spatially uncorrelated fading channel and ideal channel estimation at the receiver are assumed.

#### 4.1 Impact of the Number of Transmit Antennas

Figure 2 shows the BER performance using FD-STTD transmission with the proposed robust FDE as a function of the transmit bit energy-to-AWGN power spectrum density  $E_b/N_0$  when  $N_r = 2$  and the normalized maximum Doppler frequency  $f_D T_s = 0.0008$ . For the comparison, the BER performance using the conventional FDE, which was designed based on the assumption of a quasi-static fading, is also plotted in Fig. 2. It is seen from Fig. 2 that the BER performance when using the conventional FDE has BER error floor. This is due to the STBC codeword interference caused by the orthogonality distortion of STBC codeword. It is also seen from Fig. 2 that the proposed robust FDE achieves BER performance superior to the conventional FDE. This is because the robust FDE weights are jointly optimized taking into account not only channel frequency variation but also channel time variation over the STBC codeword and hence, it can suppress the STBC codeword interference.

It is also seen from Fig. 2 that, the BER performance of the conventional FDE is degraded by increasing the number  $N_t$  of transmit antennas from 2 to 3 while the BER performance can be improved by increasing  $N_t$  from 3 to 4. On the other hand, the BER performance of the proposed robust FDE can be improved by increasing  $N_t$  from 2 to 3 while the BER performance is degraded by increasing  $N_t$  from 3 to 4. The reason for this is explained as follows. In a high mobility environment, the FD-STTD transmission performance degrades due to not only ISI but also the STBC codeword interference. As  $N_t$  increases, the residual ISI decreases due to the increased spatial diversity gain. On the other hand, as  $N_t$  increases, STBC encoding/decoding processing becomes more complicated as indicated by Eq. (1) and (4) and therefore, the STBC codeword interference gets stronger with increasing  $N_t$  (a detailed explanation is presented in Appendix).

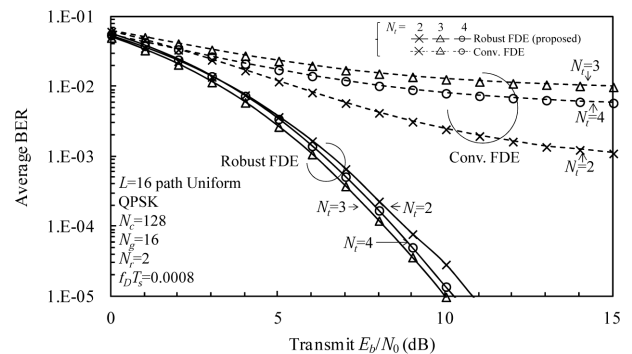


Fig. 2 Impact of the number of transmit antennas.

In the conventional FDE, FDE weight is designed without considering the channel time variation within a STBC codeword. Therefore, the channel time variation within a STBC codeword causes not only STBC codeword interference but also ISI. When increasing  $N_t$  from 2 to 3, the increase of STBC codeword interference is larger than the decrease of ISI because the STBC codeword length becomes twice longer. Therefore, the BER performance is degraded by increasing  $N_t$  from 2 to 3. On the other hand, when increasing  $N_t$  from 3 to 4, the decrease of ISI is larger than the increase of STBC codeword interference because the STBC codeword length when  $N_t = 4$  is the same as that when  $N_t = 3$ . Therefore, the BER performance can be slightly improved by increasing  $N_t$  from 3 to 4.

On the other hand, in the proposed robust FDE, FDE weights are jointly optimized considering the channel time variation within a STBC codeword and hence, the proposed robust FDE can suppress not only STBC codeword interference but also ISI caused by the channel time variation. Therefore, the robust FDE can obtain larger spatial diversity gain than the conventional FDE by increasing  $N_t$ . When increasing  $N_t$  from 2 to 3, the decrease of ISI is larger than the increase of STBC codeword interference because STBC codeword interference can be suppressed by the robust FDE. Therefore, the BER performance can be improved by increasing  $N_t$  from 2 to 3 due to the decrease of ISI. On the other hand, when  $N_t$  is more than 2, ISI is already suppressed sufficiently by spatial diversity gain and therefore, the dominant factor to degrade is STBC codeword interference. Therefore, the BER performance is slightly degraded by increasing  $N_t$  from 3 to 4 due to the increase of STBC codeword interference.

4.2 Impact of the Number of Receive Antennas

Figure 3 shows the BER performance using FD-STTD transmission with the proposed robust FDE as a function of the transmit  $E_b/N_0$  when  $N_t = 3$  and the normalized maximum Doppler frequency  $f_D T_s = 0.0008$ . It is seen from Fig. 3 that the BER performance when using the conventional receive FDE improves as the number of receive antennas increases; however, it still has BER error floor. This is due to the STBC codeword interference. On the other hand, the BER perfor-

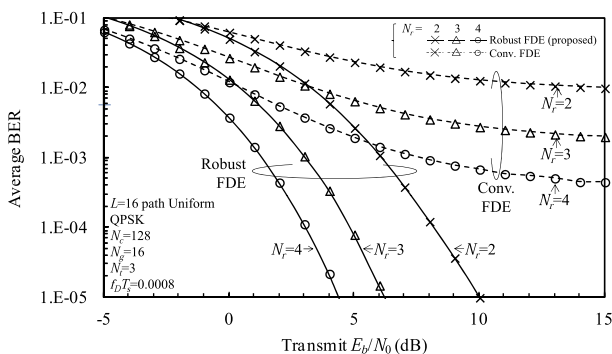


Fig. 3 Impact of the number of receive antennas.

mance when using the proposed robust FDE further improves as the number of receive antennas increases. This is because the proposed robust FDE can mitigate the STBC codeword interference and as consequence, it can obtain large spatial diversity gain even in a high mobility environment. Furthermore, in FD-STTD transmission, the STBC coding rate is independent of the number of receive antennas given as Table 1 and hence, the STBC codeword interference is constant irrespective of the number of receive antennas. Therefore, the BER performance improves as the number of receive antennas increases by spatial diversity gain. For example, setting  $N_r = 4$  can reduce the required  $E_b/N_0$  for  $BER=10^{-4}$  by about 5dB compared to when setting  $N_r = 2$ .

4.3 Impact of Doppler Frequency

Figure 4 plots the BER performance using FD-STTD transmission with the proposed robust FDE as a function of the normalized Doppler frequency  $f_D T_s$  when  $E_b/N_0 = 6$ dB and  $N_r = 2$ . It is seen from Fig. 4 that the proposed robust FDE is more robust to channel time selectivity than the conventional FDE. For example, when  $N_t = 3$  and the allowable BER is  $BER=10^{-4}$ , the proposed robust FDE can tolerate up to about 3 times higher Doppler frequency than the conventional FDE.

4.4 Comparison to Iterative Interference Cancellation

In FD-STTD transmission, the receiver requires the CSI. Using the knowledge of CSI, I<sup>2</sup>C can be applied. Figure 5 compares the BER performance of FD-STTD when using the proposed robust FDE and that when using the conventional FDE with I<sup>2</sup>C [11], [12]. The number of transmit and receive antennas are set to  $N_t = N_r = 2$ . The number  $I$  of iterations for I<sup>2</sup>C is set to  $I = 3$ . It is seen from Fig. 5 that the BER performance when using the proposed robust FDE slightly degrades compared to I<sup>2</sup>C. This is due to the residual STBC codeword interference after the robust FDE and STBC decoding. For example, the robust FDE requires about 0.7 dB larger  $E_b/N_0$  for  $BER = 10^{-4}$  than I<sup>2</sup>C. However, the performance gap between the robust FDE and I<sup>2</sup>C is sufficiently small. Table 2 compares the computational

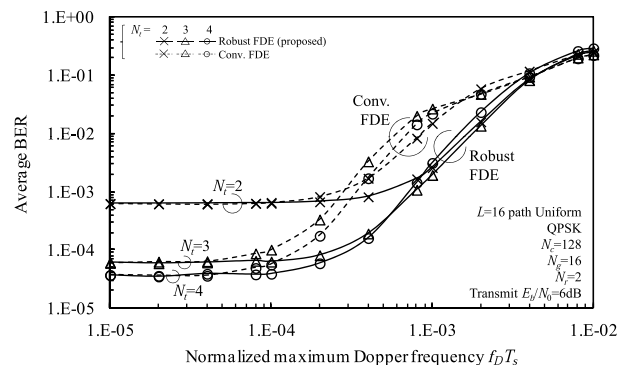


Fig. 4 Impact of normalized maximum Doppler frequency.

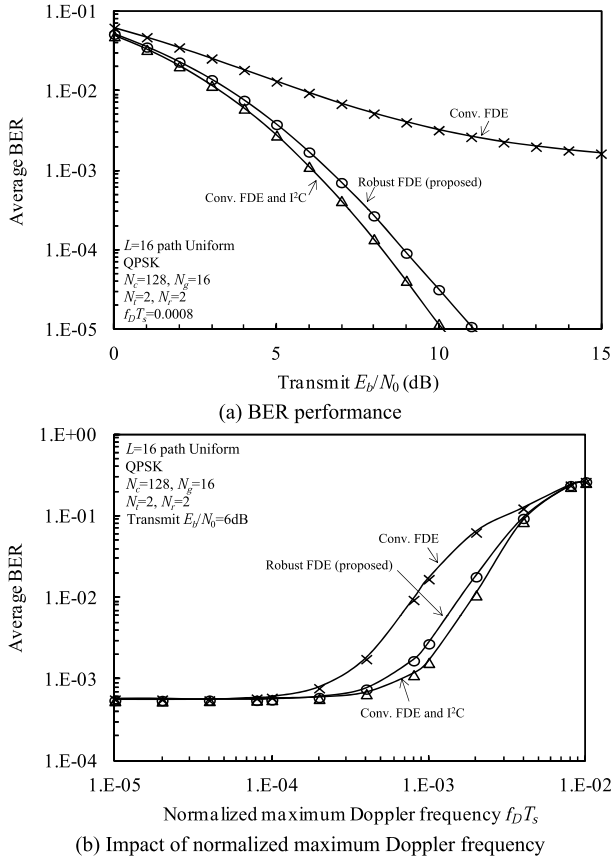


Fig. 5 Comparison to I<sup>2</sup>C.

Table 2 Computational complexity.

	Robust FDE	I <sup>2</sup> C
FFT	$QN_c \log_2 N_c$	$QN_c \log_2 N_c$
Weight computation	$N_c(16N_r+2)$	$2N_c N_r$
Weight multiplexing	$QN_r N_c$	$QN_r N_c$
IFFT	$JN_c \log_2 N_c$	$JN_c \log_2 N_c$
Replica generation		$N_c(4N_r+J)$
Overall complexity	$QN_c \log_2 N_c + N_c(16N_r+2) + QN_r N_c + JN_c \log_2 N_c$	$QN_c \log_2 N_c + 2IN_c N_r + IQN_r N_c + JN_c \log_2 N_c + IN_c(4N_r+J)$

complexity for the robust FDE and I<sup>2</sup>C when  $N_t = 2$ . In this paper, the computational complexity is defined as the number of complex number multiplications per STBC codeword. The robust FDE weights are more complicated compared to the conventional FDE as shown in Eq. (8). Therefore, the robust FDE requires larger computational complexity than the conventional FDE in order to compute FDE weights. However, the robust FDE does not require iterative processing and hence, it can reduce overall computational complexity. When  $N_r = 2$  and the number of iteration  $I = 3$ , the computational complexity for the robust FDE is 8,960 while that for I<sup>2</sup>C is 17,152. Therefore, the robust FDE can achieve almost the same BER performance with about 2 times lower computational complexity than I<sup>2</sup>C.

### 5. Conclusion

In this paper, we proposed a robust FDE for SC-STBC diversity in high mobility environment. The multiple FDE weight matrices, each associated with a different coded block, are jointly optimized based on the MMSE criterion taking into account not only channel frequency variation but also channel time variation over the STBC codeword. We showed, by computer simulation, that the proposed robust FDE always achieves better BER performance than the conventional FDE. We also showed that the proposed robust FDE can achieve almost the same BER performance with 2 times lower computational complexity than I<sup>2</sup>C.

In this paper, we consider FD-STTD transmission for the uplink transmission. FD-STTD transmission requires no CSI at the transmitter side and hence, it is suitable for the uplink transmission. On the other hand, for the downlink transmission, we consider SC-STBC diversity combined with transmit FDE proposed in Ref. [13]–[15] (called as frequency-domain space-time block coded joint transmit/receive diversity (FD-STBC-JTRD)). FD-STBC-JTRD transmission requires no CSI at the receiver side and hence, it is suitable for downlink transmission. It should be noted that our proposed robust FDE can be applied to not only FD-STTD transmission but also FD-STBC-JTRD transmission. Therefore, by using FD-STTD with the receive robust FDE for uplink and FD-STBC-JTRD with the transmit robust FDE for downlink, respectively, both uplink and downlink BER performances can be improved while reducing the computational complexity imposed on the mobile terminal even in a high mobility environment [16], [17]. Furthermore, when using time division duplex (TDD), the same frequency is reused for both uplink and downlink and hence, strong fading correlation exists between uplink fading and downlink fading. Therefore, the estimated uplink CSI can be reused for downlink transmission. No CSI feedback is necessary. However, in a very high mobility environment, the estimated uplink CSI cannot be reused for downlink transmission. This problem is left as our future study.

In this paper, spatially uncorrelated fading channel was also assumed. The impact of spatial correlation of channel is also an interesting future study.

### References

- [1] H. Sari, G. Karam, and I. Jeanclaude, "Transmission techniques for digital terrestrial TV broadcasting," *IEEE Commun. Mag.*, vol.33, no.2, pp.100–109, Feb. 1995.
- [2] D. Falconer, S.L. Ariyavisitakul, A. Benyamin-Seeyar, and B. Eidson, "Frequency domain equalization for single-carrier broadband wireless systems," *IEEE Commun. Mag.*, vol.40, no.4, pp.58–66, April 2002.
- [3] F. Adachi, H. Tomeba, and K. Takeda, "Introduction of frequency-domain signal processing to broadband single-carrier transmissions in a wireless channel," *IEICE Trans. Commun.*, vol.E92-B, no.9, pp.2789–2808, Sept. 2009.
- [4] J.G. Proakis, *Digital Communications*, 4th ed., McGraw-Hill, 2001.
- [5] R. Prasad, *OFDM for wireless communications systems*, Artech

- House, 2004.
- [6] S.H. Han and J.H. Lee, "An overview of peak-to-average power ratio reduction techniques for multicarrier transmission," *IEEE Wireless Commun.*, vol.12, no.2, pp.56–65, April 2005.
- [7] S.M. Alamouti, "A simple transmit diversity technique for wireless communications," *IEEE J. Sel. Areas. Commun.*, vol.16, no.8, pp.1451–1458, Oct. 1998.
- [8] V. Tarokh, H. Jafarkhani, and A.R. Calderbank, "Space-time block coding for wireless communications: Performance results," *IEEE J. Sel. Areas. Commun.*, vol.17, no.3, pp.451–460, March 1999.
- [9] K. Takeda, T. Itagaki and F. Adachi, "Application of space-time transmit diversity to single carrier transmission with frequency-domain equalization and receive antenna diversity in a frequency selective fading channel," *IEEE Proc. -Commun.*, vol.151, no.6, pp.627–632, Dec. 2004.
- [10] P.-H. Chiang, D.-B. Lin, and H.-J. Li, "Performance analysis of two-branch space-time block-coded DS-CDMA systems in time-varying multipath Rayleigh fading channels," *IEEE Trans. Veh. Technol.*, vol.56, no.2, pp.975–983, March 2007.
- [11] J.-W. Wee, J.-W. Seo, K.-T. Lee, Y.-S. Lee, and W.-G. Jeon, "Successive interference cancellation for STBC-OFDM systems in a fast fading channel," 2005 IEEE 61st Vehicular Technology Conference, pp.841–844, June 2005.
- [12] C.-Y. Tso, J.-M. Wu, and P.-A. Ting, "Iterative interference cancellation for STBC-OFDM systems in fast fading channels," 2009 IEEE Global Telecommunications Conference, GLOBECOM 2009, pp.1–5, 2009.
- [13] H. Tomeba, K. Takeda, and F. Adachi, "Space-time block coded joint transmit/receive diversity in a frequency-nonsselective Rayleigh fading channel," *IEICE Trans. Commun.*, vol.E89-B, no.8, pp.2189–2195, Aug. 2006.
- [14] H. Tomeba, K. Takeda, and F. Adachi, "Space-time block coded-joint transmit/receive antenna diversity using more than 4 receive antennas," *Proc. 2008 IEEE 68th Vehicular Technology Conference*, pp.1–5, 2008.
- [15] H. Tomeba, K. Takeda, and F. Adachi, "Frequency-domain space-time block coded-joint transmit/receive diversity for direct-sequence spread spectrum signal transmission," *IEICE Trans. Commun.*, vol.E90-B, no.3, pp.597–606, March 2007.
- [16] R. Matsukawa, T. Obara, and F. Adachi, "Frequency-domain space-time block coded single-carrier distributed antenna network," *IEICE Communications Express*, vol.2, no.4, pp.141–147, April 2013.
- [17] S. Yoshioka, S. Kumagai, T. Yamamoto, T. Obara, and F. Adachi, "Single-carrier STBC diversity using CDP-CE and linear inter/extrapolation in a doubly selective fading channel," *Proc. 10th IEEE VTS Asia Pacific Wireless Communications Symposium (APWCS2013)*, Seoul, Korea, Aug. 2013.
- [18] H. Miyazaki and F. Adachi, "Transmit FDE weight design for single-carrier space-time block coded joint transmit/receive diversity," *Proc. 2013 9th International Conference on Information, Communications & Signal Processing*, pp.1–5, 2013.
- [19] H. Miyazaki and F. Adachi, "Robust frequency-domain equalization against doubly selective fading for single-carrier STBC time-division duplex transmission," *Proc. 2014 International Wireless Communications and Mobile Computing Conference (IWCMC)*, pp.405–410, 2014.

#### Appendix: Derivation of the Robust FDE When $N_t = 3, 4$

(a) when  $N_t = 3$

From Eq. (1b), (2), (3) and (4b),  $e$  can be rewritten as

$$\begin{aligned}
 e = & \sum_{k=0}^{N_c-1} \left\{ \begin{aligned} & \left| \mathbf{W}_0(0, k) \mathbf{H}_0(0, k) + \mathbf{H}_1^H(1, k) \mathbf{W}_1^H(1, k) \right|^2 \\ & + \left| \mathbf{H}_2^H(2, k) \mathbf{W}_2^H(2, k) - 1 \right|^2 \\ & \left| \mathbf{W}_0(1, k) \mathbf{H}_0(1, k) + \mathbf{H}_1^H(0, k) \mathbf{W}_1^H(0, k) \right|^2 \\ & + \left| \mathbf{H}_3^H(2, k) \mathbf{W}_3^H(2, k) - 1 \right|^2 \\ & \left| \mathbf{W}_0(2, k) \mathbf{H}_0(2, k) + \mathbf{H}_2^H(0, k) \mathbf{W}_2^H(0, k) \right|^2 \\ & + \left| \mathbf{H}_3^H(1, k) \mathbf{W}_3^H(1, k) - 1 \right|^2 \end{aligned} \right\} \\
 & + N_t \left( \frac{J}{Q} \right) \left( \frac{P}{N} \right)^{-1} \sum_{k=0}^{N_c-1} \left\{ \begin{aligned} & \left\| \mathbf{W}_0(0, k) \right\|^2 + \left\| \mathbf{W}_1(1, k) \right\|^2 \\ & + \left\| \mathbf{W}_2(2, k) \right\|^2 + \left\| \mathbf{W}_0(1, k) \right\|^2 \\ & + \left\| \mathbf{W}_1(0, k) \right\|^2 + \left\| \mathbf{W}_3(2, k) \right\|^2 \\ & + \left\| \mathbf{W}_0(2, k) \right\|^2 + \left\| \mathbf{W}_2(0, k) \right\|^2 \\ & + \left\| \mathbf{W}_3(1, k) \right\|^2 \end{aligned} \right\} \\
 & + \sum_{k=0}^{N_c-1} \left\{ \begin{aligned} & \left| \mathbf{W}_0(0, k) \mathbf{H}_0(1, k) - \mathbf{H}_1^H(0, k) \mathbf{W}_1^H(1, k) \right|^2 \\ & + \left| \mathbf{W}_0(0, k) \mathbf{H}_0(2, k) - \mathbf{H}_2^H(0, k) \mathbf{W}_2^H(2, k) \right|^2 \\ & + \left| \mathbf{W}_0(1, k) \mathbf{H}_0(0, k) - \mathbf{H}_1^H(1, k) \mathbf{W}_1^H(0, k) \right|^2 \\ & + \left| \mathbf{W}_0(1, k) \mathbf{H}_0(2, k) - \mathbf{H}_3^H(1, k) \mathbf{W}_1^H(0, k) \right|^2 \\ & + \left| \mathbf{W}_0(2, k) \mathbf{H}_0(0, k) - \mathbf{H}_2^H(2, k) \mathbf{W}_2^H(0, k) \right|^2 \\ & + \left| \mathbf{W}_0(2, k) \mathbf{H}_0(1, k) - \mathbf{H}_3^H(2, k) \mathbf{W}_3^H(1, k) \right|^2 \end{aligned} \right\} \quad (\text{A} \cdot 1)
 \end{aligned}$$

The first term is the contribution of the residual ISI after STBC decoding and the second term is the contribution of the noise. The third term is the contribution of the residual STBC codeword interference. It is seen from Eq. (A.1) that the robust FDE weights,  $\mathbf{W}_1(2, k)$ ,  $\mathbf{W}_2(1, k)$  and  $\mathbf{W}_3(0, k)$  do not affect MSE  $e$ . Therefore, we obtain  $\mathbf{W}_1(2, k) = \mathbf{W}_2(1, k) = \mathbf{W}_3(0, k) = \mathbf{\Omega}(k)$  where  $\mathbf{\Omega}(k) = [\Omega(0, k), \dots, \Omega(N_t - 1, k)]^T$  with  $\Omega(n_t, k)$  being an arbitrary complex value. Furthermore, by solving  $\partial e / \partial \mathbf{W}_0(0, k) = \mathbf{0}, \dots, \partial e / \partial \mathbf{W}_{Q-1}(N_t - 1, k) = \mathbf{0}$ , the robust MMSE-FDE weights are obtained as

$$\begin{cases} \mathbf{W}_0(0, k) = \frac{\mathbf{H}_0^H(0, k) - \mathbf{H}_0^H(1, k)\alpha_0(k) + \mathbf{H}_0^H(2, k)\beta_0(k)}{\tilde{H}_{F,0}(k) - \tilde{H}_{A,0}^*(k)\alpha_0(k) + \tilde{H}_{D,0}(k)\beta_0(k)} \\ \mathbf{W}_1(1, k) = \frac{\mathbf{H}_1^H(1, k) + \mathbf{H}_1^H(0, k)\alpha_0^*(k)}{\tilde{H}_{F,0}(k) - \tilde{H}_{A,0}^*(k)\alpha_0(k) + \tilde{H}_{D,0}(k)\beta_0(k)}, \\ \mathbf{W}_2(2, k) = \frac{\mathbf{H}_2^H(2, k) - \mathbf{H}_2^H(0, k)\beta_0^*(k)}{\tilde{H}_{F,0}(k) - \tilde{H}_{A,0}^*(k)\alpha_0(k) + \tilde{H}_{D,0}(k)\beta_0(k)} \end{cases} \quad (\text{A} \cdot 2a)$$

$$\begin{cases} \mathbf{W}_0(1, k) = \frac{\mathbf{H}_0^H(1, k) - \mathbf{H}_0^H(0, k)\alpha_1(k) + \mathbf{H}_0^H(2, k)\beta_1(k)}{\tilde{H}_{F,1}(k) - \tilde{H}_{A,1}^*(k)\alpha_1(k) + \tilde{H}_{D,1}(k)\beta_1(k)} \\ \mathbf{W}_1(0, k) = \frac{\mathbf{H}_1^H(0, k) + \mathbf{H}_1^H(1, k)\alpha_1^*(k)}{\tilde{H}_{F,1}(k) - \tilde{H}_{A,1}^*(k)\alpha_1(k) + \tilde{H}_{D,1}(k)\beta_1(k)}, \\ \mathbf{W}_3(2, k) = \frac{\mathbf{H}_3^H(2, k) - \mathbf{H}_3^H(1, k)\beta_1^*(k)}{\tilde{H}_{F,1}(k) - \tilde{H}_{A,1}^*(k)\alpha_1(k) + \tilde{H}_{D,1}(k)\beta_1(k)} \end{cases} \quad (\text{A} \cdot 2b)$$

$$\begin{cases} \mathbf{W}_0(2, k) = \frac{\mathbf{H}_0^H(2, k) - \mathbf{H}_0^H(0, k)\alpha_2(k) + \mathbf{H}_0^H(1, k)\beta_2(k)}{\tilde{H}_{F,2}(k) - \tilde{H}_{A,2}^*(k)\alpha_2(k) + \tilde{H}_{D,2}^*(k)\beta_2(k)} \\ \mathbf{W}_2(0, k) = \frac{\mathbf{H}_2^H(0, k) + \mathbf{H}_2^H(2, k)\alpha_2^*(k)}{\tilde{H}_{F,2}(k) - \tilde{H}_{A,2}^*(k)\alpha_2(k) + \tilde{H}_{D,2}^*(k)\beta_2(k)}, \\ \mathbf{W}_3(1, k) = \frac{\mathbf{H}_3^H(1, k) - \mathbf{H}_3^H(2, k)\beta_2^*(k)}{\tilde{H}_{F,2}(k) - \tilde{H}_{A,2}^*(k)\alpha_2(k) + \tilde{H}_{D,2}^*(k)\beta_2(k)} \end{cases} \quad (\text{A} \cdot 2\text{c})$$

where

$$\begin{cases} \tilde{H}_{A,0}(k) = \mathbf{H}_0^H(0, k)\mathbf{H}_0(1, k) - \mathbf{H}_1^H(0, k)\mathbf{H}_1(1, k) \\ \tilde{H}_{B,0}(k) = \|\mathbf{H}_0(1, k)\|^2 + \|\mathbf{H}_1(0, k)\|^2 + N_t \left(\frac{J}{Q}\right) \left(\frac{P}{N}\right)^{-1} \\ \tilde{H}_{C,0}(k) = \mathbf{H}_0^H(2, k)\mathbf{H}_0(1, k) \\ \tilde{H}_{D,0}(k) = \mathbf{H}_0^H(0, k)\mathbf{H}_0(2, k) - \mathbf{H}_2^H(0, k)\mathbf{H}_2(2, k) \\ \tilde{H}_{E,0}(k) = \|\mathbf{H}_0(2, k)\|^2 + \|\mathbf{H}_2(0, k)\|^2 + N_t \left(\frac{J}{Q}\right) \left(\frac{P}{N}\right)^{-1}, \\ \tilde{H}_{F,0}(k) = \left\{ \begin{array}{l} \|\mathbf{H}_0(0, k)\|^2 + \|\mathbf{H}_1(1, k)\|^2 \\ + \|\mathbf{H}_2(2, k)\|^2 + N_t \left(\frac{J}{Q}\right) \left(\frac{P}{N}\right)^{-1} \end{array} \right\} \end{cases} \quad (\text{A} \cdot 3\text{a})$$

$$\begin{cases} \tilde{H}_{A,1}(k) = \mathbf{H}_0^H(1, k)\mathbf{H}_0(0, k) - \mathbf{H}_1^H(1, k)\mathbf{H}_1(0, k) \\ \tilde{H}_{B,1}(k) = \|\mathbf{H}_0(0, k)\|^2 + \|\mathbf{H}_1(1, k)\|^2 + N_t \left(\frac{J}{Q}\right) \left(\frac{P}{N}\right)^{-1} \\ \tilde{H}_{C,1}(k) = \mathbf{H}_0^H(2, k)\mathbf{H}_0(0, k) \\ \tilde{H}_{D,1}(k) = \mathbf{H}_0^H(1, k)\mathbf{H}_0(2, k) - \mathbf{H}_3^H(1, k)\mathbf{H}_3(2, k) \\ \tilde{H}_{E,1}(k) = \|\mathbf{H}_0(2, k)\|^2 + \|\mathbf{H}_3(1, k)\|^2 + N_t \left(\frac{J}{Q}\right) \left(\frac{P}{N}\right)^{-1}, \\ \tilde{H}_{F,1}(k) = \left\{ \begin{array}{l} \|\mathbf{H}_0(1, k)\|^2 + \|\mathbf{H}_1(0, k)\|^2 \\ + \|\mathbf{H}_3(2, k)\|^2 + N_t \left(\frac{J}{Q}\right) \left(\frac{P}{N}\right)^{-1} \end{array} \right\} \end{cases} \quad (\text{A} \cdot 3\text{b})$$

$$\begin{cases} \tilde{H}_{A,2}(k) = \mathbf{H}_0^H(2, k)\mathbf{H}_0(0, k) - \mathbf{H}_2^H(2, k)\mathbf{H}_2(0, k) \\ \tilde{H}_{B,2}(k) = \|\mathbf{H}_0(0, k)\|^2 + \|\mathbf{H}_2(2, k)\|^2 + N_t \left(\frac{J}{Q}\right) \left(\frac{P}{N}\right)^{-1} \\ \tilde{H}_{C,2}(k) = \mathbf{H}_0^H(1, k)\mathbf{H}_0(0, k) \\ \tilde{H}_{D,2}(k) = \mathbf{H}_0^H(2, k)\mathbf{H}_0(1, k) - \mathbf{H}_3^H(2, k)\mathbf{H}_3(1, k) \\ \tilde{H}_{E,2}(k) = \|\mathbf{H}_0(1, k)\|^2 + \|\mathbf{H}_3(2, k)\|^2 + N_t \left(\frac{J}{Q}\right) \left(\frac{P}{N}\right)^{-1}, \\ \tilde{H}_{F,2}(k) = \left\{ \begin{array}{l} \|\mathbf{H}_0(2, k)\|^2 + \|\mathbf{H}_2(0, k)\|^2 \\ + \|\mathbf{H}_3(1, k)\|^2 + N_t \left(\frac{J}{Q}\right) \left(\frac{P}{N}\right)^{-1} \end{array} \right\} \end{cases} \quad (\text{A} \cdot 3\text{c})$$

and

$$\begin{cases} \alpha_i(k) = \frac{\tilde{H}_{A,i}(k)\tilde{H}_{E,i}(k) - \tilde{H}_{C,i}(k)\tilde{H}_{D,i}(k)}{\tilde{H}_{B,i}(k)\tilde{H}_{E,i}(k) - |\tilde{H}_{C,i}(k)|^2} \\ \beta_i(k) = \frac{\tilde{H}_{A,i}(k)\tilde{H}_{C,i}^*(k) - \tilde{H}_{B,i}(k)\tilde{H}_{D,i}(k)}{\tilde{H}_{B,i}(k)\tilde{H}_{E,i}(k) - |\tilde{H}_{C,i}(k)|^2} \end{cases} \quad \text{for } i=0, 1, 2. \quad (\text{A} \cdot 4)$$

(b) when  $N_t=4$

From Eq. (1c), (2), (3) and (4c),  $e$  can be rewritten as

$$\begin{aligned} e = & \sum_{k=0}^{N_c-1} \left\{ \begin{array}{l} \left| \mathbf{W}_0(0, k)\mathbf{H}_0(0, k) + \mathbf{H}_1^H(1, k)\mathbf{W}_1^H(1, k) \right. \\ \left. + \mathbf{H}_2^H(2, k)\mathbf{W}_2^H(2, k) + \mathbf{W}_3(3, k)\mathbf{H}_3(3, k) - 1 \right|^2 \\ \left| \mathbf{W}_0(1, k)\mathbf{H}_0(1, k) + \mathbf{H}_1^H(0, k)\mathbf{W}_1^H(0, k) \right. \\ \left. + \mathbf{H}_2(3, k)\mathbf{W}_2(3, k) + \mathbf{H}_3^H(2, k)\mathbf{W}_3^H(2, k) - 1 \right|^2 \\ \left| \mathbf{W}_0(2, k)\mathbf{H}_0(2, k) + \mathbf{H}_1(3, k)\mathbf{W}_1(3, k) \right. \\ \left. + \mathbf{H}_2^H(0, k)\mathbf{W}_2^H(0, k) + \mathbf{H}_3^H(1, k)\mathbf{W}_3^H(1, k) - 1 \right|^2 \end{array} \right\} \\ & + N_t \left(\frac{J}{Q}\right) \left(\frac{P}{N}\right)^{-1} \sum_{k=0}^{N_c-1} \left\{ \begin{array}{l} \|\mathbf{W}_0(0, k)\|^2 + \|\mathbf{W}_1(1, k)\|^2 \\ + \|\mathbf{W}_2(2, k)\|^2 + \|\mathbf{W}_3(3, k)\|^2 \\ + \|\mathbf{W}_0(1, k)\|^2 + \|\mathbf{W}_1(0, k)\|^2 \\ + \|\mathbf{W}_2(3, k)\|^2 + \|\mathbf{W}_3(2, k)\|^2 \\ + \|\mathbf{W}_0(2, k)\|^2 + \|\mathbf{W}_1(3, k)\|^2 \\ + \|\mathbf{W}_2(0, k)\|^2 + \|\mathbf{W}_3(1, k)\|^2 \end{array} \right\} \\ & + \sum_{k=0}^{N_c-1} \left\{ \begin{array}{l} \left| \mathbf{W}_0(0, k)\mathbf{H}_0(1, k) - \mathbf{H}_1^H(0, k)\mathbf{W}_1^H(1, k) \right|^2 \\ + \left| \mathbf{W}_0(0, k)\mathbf{H}_0(2, k) - \mathbf{H}_2^H(0, k)\mathbf{W}_2^H(2, k) \right|^2 \\ + \left| \mathbf{W}_3(3, k)\mathbf{H}_3(2, k) - \mathbf{H}_2^H(3, k)\mathbf{W}_2^H(2, k) \right|^2 \\ + \left| \mathbf{W}_3(3, k)\mathbf{H}_3(1, k) - \mathbf{H}_1^H(3, k)\mathbf{W}_1^H(1, k) \right|^2 \\ + \left| \mathbf{W}_0(1, k)\mathbf{H}_0(0, k) - \mathbf{H}_1^H(1, k)\mathbf{W}_1^H(0, k) \right|^2 \\ + \left| \mathbf{W}_0(1, k)\mathbf{H}_0(2, k) - \mathbf{H}_3^H(1, k)\mathbf{W}_3^H(2, k) \right|^2 \\ + \left| \mathbf{W}_2(3, k)\mathbf{H}_2(2, k) - \mathbf{H}_3^H(3, k)\mathbf{W}_3^H(2, k) \right|^2 \\ + \left| \mathbf{W}_2(3, k)\mathbf{H}_2(0, k) - \mathbf{H}_1^H(3, k)\mathbf{W}_1^H(0, k) \right|^2 \\ + \left| \mathbf{W}_0(2, k)\mathbf{H}_0(0, k) - \mathbf{H}_2^H(2, k)\mathbf{W}_2^H(0, k) \right|^2 \\ + \left| \mathbf{W}_0(2, k)\mathbf{H}_0(1, k) - \mathbf{H}_3^H(2, k)\mathbf{W}_3^H(1, k) \right|^2 \\ + \left| \mathbf{W}_1(3, k)\mathbf{H}_1(1, k) - \mathbf{H}_3^H(3, k)\mathbf{W}_3^H(1, k) \right|^2 \\ + \left| \mathbf{W}_1(3, k)\mathbf{H}_1(0, k) - \mathbf{H}_2^H(3, k)\mathbf{W}_2^H(0, k) \right|^2 \end{array} \right\}. \quad (\text{A} \cdot 5)$$

The first term is the contribution of the residual ISI after STBC decoding and the second term is the contribution of the noise. The third term is the contribution of the residual STBC codeword interference. It is seen from Eq. (A.5) that the robust FDE weights,  $\mathbf{W}_0(3, k)$ ,  $\mathbf{W}_1(2, k)$ ,  $\mathbf{W}_2(1, k)$  and  $\mathbf{W}_3(0, k)$  do not affect MSE  $e$ . Therefore, we obtain  $\mathbf{W}_0(3, k) = \mathbf{W}_1(2, k) = \mathbf{W}_2(1, k) = \mathbf{W}_3(0, k) = \mathbf{\Omega}(k)$ . Furthermore, by solving  $\partial e / \partial \mathbf{W}_0(0, k) = \mathbf{0}, \dots, \partial e / \partial \mathbf{W}_{Q-1}(N_t - 1, k) = \mathbf{0}$ , the robust MMSE-FDE weights are obtained as

$$\left\{ \begin{array}{l}
\mathbf{W}_0(0, k) = \frac{\mathbf{H}_0^H(0, k) + \mathbf{H}_0^H(1, k)\alpha_0(k) + \mathbf{H}_0^H(2, k)\beta_0(k)}{\left[ \begin{array}{l} \tilde{H}_{M,0}(k) + \tilde{H}_{A,0}^*(k)\alpha_0(k) + \tilde{H}_{E,0}^*(k)\beta_0(k) \\ + \tilde{H}_{H,0}^*(k)\gamma_0(k) + \tilde{H}_{K,0}^*(k)\delta_0(k) \end{array} \right]} \\
\mathbf{W}_1(1, k) = \frac{\mathbf{H}_1^H(1, k) - \mathbf{H}_1^H(0, k)\alpha_0^*(k) - \mathbf{H}_1^H(3, k)\delta_0^*(k)}{\left[ \begin{array}{l} \tilde{H}_{M,0}(k) + \tilde{H}_{A,0}^*(k)\alpha_0(k) + \tilde{H}_{E,0}^*(k)\beta_0(k) \\ + \tilde{H}_{H,0}^*(k)\gamma_0(k) + \tilde{H}_{K,0}^*(k)\delta_0(k) \end{array} \right]} \\
\mathbf{W}_2(2, k) = \frac{\mathbf{H}_2^H(2, k) - \mathbf{H}_2^H(0, k)\beta_0^*(k) - \mathbf{H}_2^H(3, k)\gamma_0^*(k)}{\left[ \begin{array}{l} \tilde{H}_{M,0}(k) + \tilde{H}_{A,0}^*(k)\alpha_0(k) + \tilde{H}_{E,0}^*(k)\beta_0(k) \\ + \tilde{H}_{H,0}^*(k)\gamma_0(k) + \tilde{H}_{K,0}^*(k)\delta_0(k) \end{array} \right]}, \\
\mathbf{W}_3(3, k) = \frac{\mathbf{H}_3^H(3, k) + \mathbf{H}_3^H(2, k)\gamma_0(k) + \mathbf{H}_3^H(1, k)\delta_0(k)}{\left[ \begin{array}{l} \tilde{H}_{M,0}(k) + \tilde{H}_{A,0}^*(k)\alpha_0(k) + \tilde{H}_{E,0}^*(k)\beta_0(k) \\ + \tilde{H}_{H,0}^*(k)\gamma_0(k) + \tilde{H}_{K,0}^*(k)\delta_0(k) \end{array} \right]}
\end{array} \right. \quad (\text{A} \cdot 6\text{a})$$

$$\left\{ \begin{array}{l}
\mathbf{W}_0(1, k) = \frac{\mathbf{H}_0^H(1, k) + \mathbf{H}_0^H(0, k)\alpha_1(k) + \mathbf{H}_0^H(2, k)\beta_1(k)}{\left[ \begin{array}{l} \tilde{H}_{M,1}(k) + \tilde{H}_{A,1}^*(k)\alpha_1(k) + \tilde{H}_{E,1}^*(k)\beta_1(k) \\ + \tilde{H}_{H,1}^*(k)\gamma_1(k) + \tilde{H}_{K,1}^*(k)\delta_1(k) \end{array} \right]} \\
\mathbf{W}_1(0, k) = \frac{\mathbf{H}_1^H(0, k) - \mathbf{H}_1^H(1, k)\alpha_1^*(k) - \mathbf{H}_1^H(3, k)\delta_1^*(k)}{\left[ \begin{array}{l} \tilde{H}_{M,1}(k) + \tilde{H}_{A,1}^*(k)\alpha_1(k) + \tilde{H}_{E,1}^*(k)\beta_1(k) \\ + \tilde{H}_{H,1}^*(k)\gamma_1(k) + \tilde{H}_{K,1}^*(k)\delta_1(k) \end{array} \right]} \\
\mathbf{W}_3(2, k) = \frac{\mathbf{H}_3^H(2, k) - \mathbf{H}_3^H(1, k)\beta_1^*(k) - \mathbf{H}_3^H(3, k)\gamma_1^*(k)}{\left[ \begin{array}{l} \tilde{H}_{M,1}(k) + \tilde{H}_{A,1}^*(k)\alpha_1(k) + \tilde{H}_{E,1}^*(k)\beta_1(k) \\ + \tilde{H}_{H,1}^*(k)\gamma_1(k) + \tilde{H}_{K,1}^*(k)\delta_1(k) \end{array} \right]}, \\
\mathbf{W}_2(3, k) = \frac{\mathbf{H}_2^H(3, k) + \mathbf{H}_2^H(2, k)\gamma_1(k) + \mathbf{H}_2^H(0, k)\delta_1(k)}{\left[ \begin{array}{l} \tilde{H}_{M,1}(k) + \tilde{H}_{A,1}^*(k)\alpha_1(k) + \tilde{H}_{E,1}^*(k)\beta_1(k) \\ + \tilde{H}_{H,1}^*(k)\gamma_1(k) + \tilde{H}_{K,1}^*(k)\delta_1(k) \end{array} \right]}
\end{array} \right. \quad (\text{A} \cdot 6\text{b})$$

$$\left\{ \begin{array}{l}
\mathbf{W}_0(2, k) = \frac{\mathbf{H}_0^H(2, k) + \mathbf{H}_0^H(0, k)\alpha_2(k) + \mathbf{H}_0^H(1, k)\beta_2(k)}{\left[ \begin{array}{l} \tilde{H}_{M,2}(k) + \tilde{H}_{A,2}^*(k)\alpha_2(k) + \tilde{H}_{E,2}^*(k)\beta_2(k) \\ + \tilde{H}_{H,2}^*(k)\gamma_2(k) + \tilde{H}_{K,2}^*(k)\delta_2(k) \end{array} \right]} \\
\mathbf{W}_2(0, k) = \frac{\mathbf{H}_2^H(0, k) - \mathbf{H}_2^H(2, k)\alpha_2^*(k) - \mathbf{H}_2^H(3, k)\delta_2^*(k)}{\left[ \begin{array}{l} \tilde{H}_{M,2}(k) + \tilde{H}_{A,2}^*(k)\alpha_2(k) + \tilde{H}_{E,2}^*(k)\beta_2(k) \\ + \tilde{H}_{H,2}^*(k)\gamma_2(k) + \tilde{H}_{K,2}^*(k)\delta_2(k) \end{array} \right]} \\
\mathbf{W}_3(1, k) = \frac{\mathbf{H}_3^H(1, k) - \mathbf{H}_3^H(2, k)\beta_2^*(k) - \mathbf{H}_3^H(3, k)\gamma_2^*(k)}{\left[ \begin{array}{l} \tilde{H}_{M,2}(k) + \tilde{H}_{A,2}^*(k)\alpha_2(k) + \tilde{H}_{E,2}^*(k)\beta_2(k) \\ + \tilde{H}_{H,2}^*(k)\gamma_2(k) + \tilde{H}_{K,2}^*(k)\delta_2(k) \end{array} \right]}, \\
\mathbf{W}_1(3, k) = \frac{\mathbf{H}_1^H(3, k) + \mathbf{H}_1^H(1, k)\gamma_2(k) + \mathbf{H}_1^H(0, k)\delta_2(k)}{\left[ \begin{array}{l} \tilde{H}_{M,2}(k) + \tilde{H}_{A,2}^*(k)\alpha_2(k) + \tilde{H}_{E,2}^*(k)\beta_2(k) \\ + \tilde{H}_{H,2}^*(k)\gamma_2(k) + \tilde{H}_{K,2}^*(k)\delta_2(k) \end{array} \right]}
\end{array} \right. \quad (\text{A} \cdot 6\text{c})$$

where

$$\left\{ \begin{array}{l}
\tilde{H}_{A,0}(k) = \mathbf{H}_0^H(0, k)\mathbf{H}_0(1, k) - \mathbf{H}_1^H(0, k)\mathbf{H}_1(1, k) \\
\tilde{H}_{B,0}(k) = \|\mathbf{H}_0(1, k)\|^2 + \|\mathbf{H}_1(0, k)\|^2 + N_t \left( \frac{J}{Q} \right) \left( \frac{P}{N} \right)^{-1} \\
\tilde{H}_{C,0}(k) = \mathbf{H}_0^H(2, k)\mathbf{H}_0(1, k) \\
\tilde{H}_{D,0}(k) = \mathbf{H}_1^H(0, k)\mathbf{H}_1(3, k) \\
\tilde{H}_{E,0}(k) = \mathbf{H}_0^H(0, k)\mathbf{H}_0(2, k) - \mathbf{H}_2^H(0, k)\mathbf{H}_2(2, k) \\
\tilde{H}_{F,0}(k) = \|\mathbf{H}_0(2, k)\|^2 + \|\mathbf{H}_2(0, k)\|^2 + N_t \left( \frac{J}{Q} \right) \left( \frac{P}{N} \right)^{-1} \\
\tilde{H}_{G,0}(k) = \mathbf{H}_2^H(0, k)\mathbf{H}_2(3, k) \\
\tilde{H}_{H,0}(k) = \mathbf{H}_3^H(3, k)\mathbf{H}_3(2, k) - \mathbf{H}_2^H(3, k)\mathbf{H}_2(2, k) \\
\tilde{H}_{I,0}(k) = \|\mathbf{H}_3(2, k)\|^2 + \|\mathbf{H}_2(3, k)\|^2 + N_t \left( \frac{J}{Q} \right) \left( \frac{P}{N} \right)^{-1} \\
\tilde{H}_{J,0}(k) = \mathbf{H}_3^H(1, k)\mathbf{H}_3(2, k) \\
\tilde{H}_{K,0}(k) = \mathbf{H}_3^H(3, k)\mathbf{H}_3(1, k) - \mathbf{H}_1^H(3, k)\mathbf{H}_1(1, k) \\
\tilde{H}_{L,0}(k) = \|\mathbf{H}_3(1, k)\|^2 + \|\mathbf{H}_1(3, k)\|^2 + N_t \left( \frac{J}{Q} \right) \left( \frac{P}{N} \right)^{-1} \\
\tilde{H}_{M,0}(k) = \left\{ \begin{array}{l} \|\mathbf{H}_0(0, k)\|^2 + \|\mathbf{H}_1(1, k)\|^2 + \|\mathbf{H}_2(2, k)\|^2 \\ + \|\mathbf{H}_3(3, k)\|^2 + N_t \left( \frac{J}{Q} \right) \left( \frac{P}{N} \right)^{-1} \end{array} \right\}
\end{array} \right. \quad (\text{A} \cdot 7\text{a})$$

$$\left\{ \begin{array}{l}
\tilde{H}_{A,1}(k) = \mathbf{H}_0^H(1, k)\mathbf{H}_0(0, k) - \mathbf{H}_1^H(1, k)\mathbf{H}_1(0, k) \\
\tilde{H}_{B,1}(k) = \|\mathbf{H}_0(0, k)\|^2 + \|\mathbf{H}_1(1, k)\|^2 + N_t \left( \frac{J}{Q} \right) \left( \frac{P}{N} \right)^{-1} \\
\tilde{H}_{C,1}(k) = \mathbf{H}_0^H(2, k)\mathbf{H}_0(0, k) \\
\tilde{H}_{D,1}(k) = \mathbf{H}_1^H(1, k)\mathbf{H}_1(3, k) \\
\tilde{H}_{E,1}(k) = \mathbf{H}_0^H(1, k)\mathbf{H}_0(2, k) - \mathbf{H}_3^H(1, k)\mathbf{H}_3(2, k) \\
\tilde{H}_{F,1}(k) = \|\mathbf{H}_0(2, k)\|^2 + \|\mathbf{H}_3(1, k)\|^2 + N_t \left( \frac{J}{Q} \right) \left( \frac{P}{N} \right)^{-1} \\
\tilde{H}_{G,1}(k) = \mathbf{H}_3^H(1, k)\mathbf{H}_3(3, k) \\
\tilde{H}_{H,1}(k) = \mathbf{H}_2^H(3, k)\mathbf{H}_2(2, k) - \mathbf{H}_3^H(3, k)\mathbf{H}_3(2, k) \\
\tilde{H}_{I,1}(k) = \|\mathbf{H}_2(2, k)\|^2 + \|\mathbf{H}_3(3, k)\|^2 + N_t \left( \frac{J}{Q} \right) \left( \frac{P}{N} \right)^{-1} \\
\tilde{H}_{J,1}(k) = \mathbf{H}_2^H(0, k)\mathbf{H}_2(2, k) \\
\tilde{H}_{K,1}(k) = \mathbf{H}_2^H(3, k)\mathbf{H}_2(0, k) - \mathbf{H}_1^H(3, k)\mathbf{H}_1(0, k) \\
\tilde{H}_{L,1}(k) = \|\mathbf{H}_2(0, k)\|^2 + \|\mathbf{H}_1(3, k)\|^2 + N_t \left( \frac{J}{Q} \right) \left( \frac{P}{N} \right)^{-1} \\
\tilde{H}_{M,1}(k) = \left\{ \begin{array}{l} \|\mathbf{H}_0(1, k)\|^2 + \|\mathbf{H}_1(0, k)\|^2 + \|\mathbf{H}_2(3, k)\|^2 \\ + \|\mathbf{H}_3(2, k)\|^2 + N_t \left( \frac{J}{Q} \right) \left( \frac{P}{N} \right)^{-1} \end{array} \right\}
\end{array} \right. \quad (\text{A} \cdot 7\text{b})$$

$$\left\{ \begin{array}{l}
\tilde{H}_{A,2}(k) = \mathbf{H}_0^H(2, k)\mathbf{H}_0(0, k) - \mathbf{H}_2^H(2, k)\mathbf{H}_2(0, k) \\
\tilde{H}_{B,2}(k) = \|\mathbf{H}_0(0, k)\|^2 + \|\mathbf{H}_2(2, k)\|^2 + N_t \left(\frac{J}{Q}\right) \left(\frac{P}{N}\right)^{-1} \\
\tilde{H}_{C,2}(k) = \mathbf{H}_0^H(1, k)\mathbf{H}_0(0, k) \\
\tilde{H}_{D,2}(k) = \mathbf{H}_2^H(2, k)\mathbf{H}_2(3, k) \\
\tilde{H}_{E,2}(k) = \mathbf{H}_0^H(2, k)\mathbf{H}_0(1, k) - \mathbf{H}_3^H(2, k)\mathbf{H}_3(1, k) \\
\tilde{H}_{F,2}(k) = \|\mathbf{H}_0(1, k)\|^2 + \|\mathbf{H}_3(2, k)\|^2 + N_t \left(\frac{J}{Q}\right) \left(\frac{P}{N}\right)^{-1} \\
\tilde{H}_{G,2}(k) = \mathbf{H}_3^H(2, k)\mathbf{H}_3(3, k) \\
\tilde{H}_{H,2}(k) = \mathbf{H}_1^H(3, k)\mathbf{H}_1(1, k) - \mathbf{H}_3^H(3, k)\mathbf{H}_3(1, k) \\
\tilde{H}_{I,2}(k) = \|\mathbf{H}_1(1, k)\|^2 + \|\mathbf{H}_3(3, k)\|^2 + N_t \left(\frac{J}{Q}\right) \left(\frac{P}{N}\right)^{-1} \\
\tilde{H}_{J,2}(k) = \mathbf{H}_1^H(0, k)\mathbf{H}_1(1, k) \\
\tilde{H}_{K,2}(k) = \mathbf{H}_1^H(3, k)\mathbf{H}_1(0, k) - \mathbf{H}_2^H(3, k)\mathbf{H}_2(0, k) \\
\tilde{H}_{L,2}(k) = \|\mathbf{H}_1(0, k)\|^2 + \|\mathbf{H}_2(3, k)\|^2 + N_t \left(\frac{J}{Q}\right) \left(\frac{P}{N}\right)^{-1} \\
\tilde{H}_{M,2}(k) = \left\{ \begin{array}{l}
\|\mathbf{H}_0(2, k)\|^2 + \|\mathbf{H}_1(3, k)\|^2 + \|\mathbf{H}_2(0, k)\|^2 \\
+ \|\mathbf{H}_3(1, k)\|^2 + N_t \left(\frac{J}{Q}\right) \left(\frac{P}{N}\right)^{-1}
\end{array} \right\}
\end{array} \right. \quad (\text{A} \cdot 7\text{c})$$

Furthermore,  $\alpha_i(k)$ ,  $\beta_i(k)$ ,  $\gamma_i(k)$  and  $\delta_i(k)$  ( $i=0, 1, 2$ ) satisfy the following equations given as

$$\left\{ \begin{array}{l}
\tilde{H}_{A,i}(k) + \tilde{H}_{B,i}(k)\alpha_i(k) + \tilde{H}_{C,i}(k)\beta_i(k) + \tilde{H}_{D,i}(k)\delta_i(k) = 0 \\
\tilde{H}_{E,i}(k) + \tilde{H}_{C,i}^*(k)\alpha_i(k) + \tilde{H}_{F,i}(k)\beta_i(k) + \tilde{H}_{B,i}(k)\gamma_i(k) = 0 \\
\tilde{H}_{H,i}(k) + \tilde{H}_{G,i}^*(k)\alpha_i(k) + \tilde{H}_{I,i}(k)\gamma_i(k) + \tilde{H}_{J,i}(k)\delta_i(k) = 0 \\
\tilde{H}_{K,i}(k) + \tilde{H}_{D,i}^*(k)\alpha_i(k) + \tilde{H}_{J,i}^*(k)\gamma_i(k) + \tilde{H}_{L,i}(k)\delta_i(k) = 0
\end{array} \right. \quad (\text{A} \cdot 8)$$

It is understood from Eq. (11), (A·1) and (A·5) that the residual STBC codeword interference after the robust FDE gets stronger as  $N_t$  increases. This is because STBC encoding/decoding processing becomes more complicated as  $N_t$  increases indicated by Eq. (1) and (4).



**Hiroyuki Miyazaki** received his B.S. degree in Information and Intelligent Systems in 2011 and M.S. degree in Electrical and Communications Engineering, in 2013, respectively, from Tohoku University, Sendai Japan. Currently he is a Japan Society for the Promotion of Science (JSPS) research fellow, studying toward his PhD degree at the Department of Communications Engineering, Graduate School of Engineering, Tohoku University. His research interests include space-time block coding for mobile communication systems. He was a recipient of 2013 IEICE RCS (Radio Communication Systems) Active Research Award.



**Fumiya Adachi** received the B.S. and Dr. Eng. degrees in electrical engineering from Tohoku University, Sendai, Japan, in 1973 and 1984, respectively. In April 1973, he joined the Electrical Communications Laboratories of Nippon Telegraph & Telephone Corporation (now NTT) and conducted various types of research related to digital cellular mobile communications. From July 1992 to December 1999, he was with NTT Mobile Communications Network, Inc. (now NTT DoCoMo, Inc.), where

he led a research group on wideband/broadband CDMA wireless access for IMT-2000 and beyond. Since January 2000, he has been with Tohoku University, Sendai, Japan, where he is a distinguished Professor of Communications Engineering at the Graduate School of Engineering. His research interest is in the areas of wireless signal processing and networking including broadband wireless access, equalization, transmit/receive antenna diversity, MIMO, adaptive transmission, channel coding, etc. He was a program leader of the 5-year Global COE Program "Center of Education and Research for Information Electronics Systems" (2007–2011), awarded by the Ministry of Education, Culture, Sports, Science and Technology of Japan. From October 1984 to September 1985, he was a United Kingdom SERC Visiting Research Fellow in the Department of Electrical Engineering and Electronics at Liverpool University. He is an IEICE Fellow and was a co-recipient of the IEICE Transactions best paper of the year award 1996, 1998, and 2009 and also a recipient of Achievement award 2003. He is an IEEE Fellow and a VTS Distinguished Lecturer for 2011 to 2013. He was a co-recipient of the IEEE Vehicular Technology Transactions best paper of the year award 1980 and again 1990 and also a recipient of Avant Garde award 2000. He was a recipient of Thomson Scientific Research Front Award 2004, Ericsson Telecommunications Award 2008, Telecom System Technology Award 2009, and Prime Minister Invention Prize 2010.